Compliance Control for an Anthropomorphic Robot with Elastic Joints: Theory and Experiments

Loredana Zollo[1], Bruno Siciliano[2], Alessandro De Luca[3], Eugenio Guglielmelli[1], Paolo Dario[1]

[1] *Scuola Superiore Sant'Anna*
ARTS Lab — c/o Polo Sant'Anna Valdera
Viale Rinaldo Piaggio 34, 56025 Pontedera (Pisa), Italy
Tel.: +39-050-883400; fax: +39-050-883497
Email: {l.zollo, e.guglielmelli, p.dario}@arts.sssup.it

[2] *PRISMA Lab*
Dipartimento di Informatica e Sistemistica
Università degli Studi di Napoli Federico II
Via Claudio 21, 80125 Napoli, Italy
Tel.: +39-081-7683179; fax: +39-062-33226128
Email: siciliano@unina.it

[3] *Dipartimento di Informatica e Sistemistica*
Università degli Studi di Roma "La Sapienza"
Via Eudossiana 18
00184 Roma, Italy
Tel.: +39-06-44585371; fax: +39-06-44585367
Email: deluca@dis.uniroma1.it

Abstract

Studies on motion control of robot manipulators with elastic joints are basically aimed at improving robot performance in tracking or regulation tasks. In the interaction between robots and environment, instead, the main objective of a control strategy should be the reduction of the vibrational and chattering phenomena that elasticity in the robot joints can cause. This work takes into account working environments where unexpected interactions are experienced and proposes a compliance control scheme in the Cartesian space to reduce the counter effects of elasticity. Two theoretical formulations of the control law are presented, which differ for the term of gravity compensation. For both of them the closed-loop equilibrium conditions are evaluated and asymptotic stability is proven through the direct Lyapunov method. The two control laws are applied to a particular class of elastic robot manipulators, i.e. cable-actuated robots, since their intrinsic mechanical compliance can be successfully utilized in applications of biomedical robotics and assistive robotics. A compared experimental analysis of the two formulations of compliance control is finally carried out in order to verify stability of the two closed-loop systems as well as the capability to control the robot force in the interaction.

1 Introduction

In many application fields, from industrial robotics up to biomedical or assistive robotics, where a very close human-robot interaction is needed, one can resort to suitable mechanical solutions to increase the level of safety and reliability in situations of unpredictable contacts of robot manipulators with the environment, e.g. by adopting lightweight structures.

One approach to the mechanical design of lightweight manipulators is based on the use of low inertia actuators, as in the distributed elastically coupled macro-mini parallel actuation [1]. This system has the purpose of ensuring high performance in position tracking tasks as well as in interaction tasks, through a micro system driven by stiff transmissions and low inertia actuators.

Using compliant elements in the mechanical transmission system can be regarded as another approach to the design of safe robots. In particular, if the intrinsic compliance can be considered as concentrated at the joints, the assumption of robots with elastic joints can be made. This is the case of robot manipulators actuated through pulleys and steel cables, where the elasticity is determined by the elastic coefficient of the cables. Cable actuation can ensure human-like dimensions of the artifact, lightness and also anthropomorphic mass distribution, which are fundamental requirements for biomedical and assistive robotics [2]–[4].

Control algorithms conceived for completely rigid robots may guarantee a stable behavior even if a certain degree of elasticity in the actuation system and motor transmission elements, or in the link structure, is present [5], [6]. The price to pay, however, is a typical degradation of robot performance. In fact, elasticity of mechanical transmissions induces position errors at the robot's end effector because of static deformation under gravity. In addition, it may generate lightly damped vibrational modes, which reduce robot accuracy in tracking tasks [5]. Yet, it may become a source of instability in case of interaction between the robot and the environment [7], possibly leading to undesirable effects of chattering during contact [8].

Several solutions have been proposed in the literature to cope with the control issue of robot manipulators with rigid joints interacting with the working environment. They range from the concept of active compliance to the concept of making the robot's end effector to behave as a mechanical impedance (see e.g. [9] for a survey), up to the hybrid position/force control approach [10].

On the other hand, the dynamic effects of elasticity in the joints have been extensively studied for improving robot performance in regulation and tracking tasks [11]. To this regard, classical techniques used for rigid

robots, input-output decoupling, feedback linearization or else inversion control, have been revisited.

For trajectory tracking control, one has to resort to a nonlinear static state feedback or to an approximate singular perturbation model of elastic joint manipulator dynamics [12] when a reduced model of the robot can be used [13], whereas a nonlinear dynamic state feedback is needed in the case of a complete dynamic model [14]. Whenever regulation is desired, instead, a simple PD control plus gravity compensation in the joint space can be adopted, as proposed in [15].

The problem of controlling robot manipulators with elastic joints in situations of interaction with the working environment, instead, is not widely dealt within the literature.

The PD control proposed in [15] can be regarded as a feasible interaction control since it provides a sort of compliance at joints if the feedback gains are properly adjusted. On the other hand, the singularly perturbed model can be suitably exploited to achieve force control either in a hybrid position/force control or impedance control framework [16], or when a constraint on the environment is present [17]. This control approach allows compensating for joint flexibility by introducing a corrective torque input.

Nevertheless, it should be stressed that all the interaction control schemes for robots with elastic joints proposed in the literature are validated by means of simulation tests on 2- or 3-degree-of-freedom (d.o.f.) manipulators.

This paper is aimed at presenting a complete theoretical formulation of a compliance control in the Cartesian space plus gravity compensation for robots with elastic joints. The controller consists of a proportional-derivative action plus gravity compensation, as for rigid robots, but a new position variable, named the gravity-biased motor position, is introduced [18]. This allows using only the position and velocity information, available from the position sensors on the rotors, to achieve an easy regulation of compliance in the Cartesian space. Asymptotic stability is proven for two formulations of the control law, namely, compliance control with constant gravity compensation (as in [15]), and compliance control with on-line gravity compensation.

Further, the two control laws are experimentally tested on an 8-d.o.f. cable-driven robot manipulator in order to verify stability of the closed-loop system and also the capability of force accommodation, by measuring the interaction force for different sets of proportional gains. A comparison of the experimental results is finally provided.

2 Robot dynamic model

Robot manipulators with n moving rigid links driven by electrical motors through n joints/transmissions subject to small elastic deformations are considered.

Under the assumptions in [13], the dynamic model of a robot with elastic joints can be expressed as

$$M(q)\ddot{q} + S(q,\dot{q})\dot{q} + g(q) + K(q-\theta) = 0 \tag{1}$$

$$I\ddot{\theta} + K(\theta - q) = u \tag{2}$$

where q is the $(n \times 1)$ vector of link positions and θ is the $(n \times 1)$ vector of motor positions reflected through the gear reductions. It is assumed that only the motor variables θ and $\dot{\theta}$ are measurable, or the latter are possibly obtained by accurate numerical differentiation.

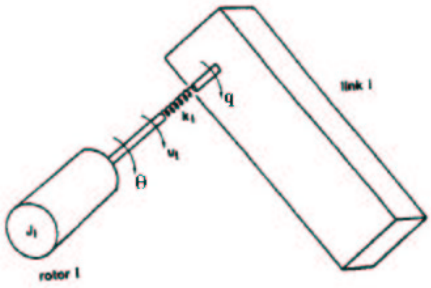

Figure 1: *Elastic joint*

In (1), $M(q)$ is the $(n \times n)$ robot link inertia matrix, $S(q,\dot{q})\dot{q}$ is the $(n \times 1)$ vector of centrifugal and Coriolis torques, K is the $(n \times n)$ diagonal matrix of joint stiffness coefficients, and $g(q) = \left(\frac{\partial U_g(q)}{\partial q}\right)^T$ is the $(n \times 1)$ vector of gravitational torque, where $U_g(q)$ is the potential energy due to gravity. Also, in (2) I is an $(n \times n)$ constant diagonal matrix including the rotor inertia and the gear ratios.

The robot dynamic model (1), (2) presents three important properties which will be useful in the demonstration of asymptotic stability of the control law.

P1. The inertia matrix $M(q)$ is symmetric and positive definite for all q.

P2. If a representation in Christoffel symbols is chosen for the elements of $S(q,\dot{q})$, the matrix $\dot{M} - 2S$ is skew-symmetric.

P3. A positive constant α exists such that

$$\left\| \frac{\partial g(q)}{\partial q} \right\| = \left\| \frac{\partial^2 U_g(q)}{\partial q^2} \right\| \leq \alpha \tag{3}$$

where the matrix norm of a symmetric matrix $A(q)$ is given by $\lambda_{\max}(A(q))$, i.e., its largest (real) eigenvalue at q[1]. Inequality (3) holds for all q and implies

$$\| g(q_1) - g(q_2)\| \leq \alpha \|q_1 - q_2\|, \tag{4}$$

for any q_1, q_2. It should be explicitly remarked that this inequality holds whatever argument is used for evaluating the gravity vector.

3 Compliance control with constant gravity compensation

Let x be the $(m \times 1)$ task vector (i.e. the Cartesian end-effector pose), with $m \leq n$, and x_d its desired constant value. The direct and differential kinematics are, respectively,

$$x = x(q), \qquad \dot{x} = J(q)\dot{q} \tag{5}$$

and depend on the link position variables only. The matrix $J(q)$ is the analytical robot Jacobian matrix. If $m = n$ and away from singularities, a finite number of inverse kinematics solutions q_d is associated with x_d, i.e., such that $x(q_d) = x_d$. Since, in general, singular configurations are to be avoided, i.e., $\det J(q_d) \neq 0$, the vector q_d has to be selected in the same class of inverse kinematics solutions as the initial configuration q_0. If $m < n$, ∞^{n-m} inverse kinematics solutions q_d exist and some of them can be singular ($\operatorname{rank} J(q_d) < m$). Also in this case, a nonsingular inverse kinematic solution has to be selected as q_d.

In [15], a PD control in the joint space is proposed for regulation tasks of robots with elastic joints. Indeed, it could be adapted to interaction situations if the matrix of joint proportional gains is varied to regulate robot compliance. In what follows, the control is extended to the Cartesian space in order to perform regulation tasks as well as to modulate robot compliance at the end effector.

The control law is

$$u = J^T(\tilde{\theta})K_P \left(x_d - x(\tilde{\theta})\right) - K_D\dot{\theta} + g(q_d), \tag{6}$$

which provides the torque vector u of the robot dynamic model (1), (2) as a combination of a proportional term, acting on the Cartesian error, a motor damping (derivative) term, and a constant compensation of gravity at the desired q_d. The $(m \times m)$ matrix K_P and the $(n \times n)$ matrix K_D are positive definite and set the proportional and derivative gains, while the $(n \times 1)$ vector

$$\tilde{\theta} = \theta - K^{-1}g(q_d) \tag{7}$$

[1]This is the matrix norm naturally induced by the Euclidean norm on vectors, e.g., $\|q\| = \sqrt{\sum_{i=1}^{n} q_i^2}$.

is a 'gravity-biased' modification of the measured motor position θ.

It is worth noting that the kinematic terms $x(\tilde{\theta})$ (direct kinematics) and $J^T(\tilde{\theta})$ (Jacobian transpose) are evaluated as a function of $\tilde{\theta}$ (instead of the argument q); the rationale is that, as shown afterwards, these expressions shall provide the correct values at steady state, even without a direct measure of q. As a matter of fact, the control law (6) can be implemented using only motor variables.

3.1 Closed-loop equilibria

The equilibrium configurations of the closed-loop system (1), (2), (6) are computed by setting $\dot{q} \equiv \dot{\theta} \equiv 0$. This yields

$$g(q) + K(q - \theta) = 0 \tag{8}$$

$$K(\theta - q) = J^T(\tilde{\theta}) K_P \left(x_d - x(\tilde{\theta}) \right) + g(q_d). \tag{9}$$

From (8) it follows that, at any equilibrium, $\theta = q + K^{-1} g(q)$. Then, adding (8) to (9) leads to

$$J^T(q + K^{-1}(g(q) - g(q_d))) K_P \left(x_d - x(q + K^{-1}(g(q) - g(q_d))) \right) + g(q_d) - g(q) = 0. \tag{10}$$

Indeed

$$q = q_d \quad \text{and thus} \quad \theta = q_d + K^{-1} g(q_d) := \theta_d \tag{11}$$

is a closed-loop equilibrium configuration. Moreover, in correspondence of this equilibrium, $\tilde{\theta}_d := \theta_d - K^{-1} g(q_d) = q_d$ and consequently $x(\tilde{\theta}_d) = x_d$.

In the assumption of $m = n$, i.e., the robot is not kinematically redundant for the considered task, the uniqueness of such equilibrium is now shown under a mild additional assumption. Adding to both (8) and (9) the term $K(\theta_d - q_d) - g(q_d) = 0$ leads to

$$K(q - q_d) - K(\theta - \theta_d) + g(q) - g(q_d) = 0 \tag{12}$$

$$-K(q - q_d) + K(\theta - \theta_d) + J^T(\tilde{\theta}) K_P \Big(x(\tilde{\theta}) - x_d \Big) = 0 \tag{13}$$

where the sign of the last equation has been changed. The following expansion holds true

$$\begin{aligned} x(\tilde{\theta}) - x_d &= x\left(q_d + (\theta - \theta_d)\right) - x_d = x(q_d) + J(q_d)(\theta - \theta_d) + o(\|\theta - \theta_d\|^2) - x_d \\ &= J\left(\tilde{\theta} + (\theta_d - \theta)\right)(\theta - \theta_d) + o(\|\theta - \theta_d\|^2) = J(\tilde{\theta})(\theta - \theta_d) + o_1(\|\theta - \theta_d\|^2). \end{aligned}$$

Therefore, Equations (12) and (13) can be rearranged as

$$\begin{bmatrix} K & -K \\ -K & K + J^T(\tilde{\theta}) K_P J(\tilde{\theta}) \end{bmatrix} \begin{bmatrix} q - q_d \\ \theta - \theta_d \end{bmatrix} = \begin{bmatrix} g(q_d) - g(q) \\ o_1(\|\theta - \theta_d\|^2) \end{bmatrix}. \tag{14}$$

Away from kinematic singularities, the smallest (real) eigenvalue $\lambda_{\min}(\bar{K})$ of the symmetric matrix

$$\bar{K} = \begin{bmatrix} K & -K \\ -K & K + J^T(\tilde{\theta}) K_P J(\tilde{\theta}) \end{bmatrix} \tag{15}$$

can be always bounded away from zero. In fact, in the above assumptions, a sufficiently large (diagonal) K_P can be always selected such that

$$\lambda_{\min}\left(\bar{K}\right) > \alpha. \tag{16}$$

As a consequence, using the inequality (4) extracted by property **P3** leads to

$$\begin{aligned} \left\| \begin{bmatrix} K & -K \\ -K & K + J^T(\tilde{\theta}) K_P J(\tilde{\theta}) \end{bmatrix} \begin{bmatrix} q - q_d \\ \theta - \theta_d \end{bmatrix} \right\| &\geq \lambda_{\min}\left(\bar{K}\right) \left\| \begin{bmatrix} q - q_d \\ \theta - \theta_d \end{bmatrix} \right\| \geq \lambda_{\min}\left(\bar{K}\right) \|q - q_d\| \\ &> \alpha \|q - q_d\| \geq \|g(q_d) - g(q)\| \end{aligned} \tag{17}$$

and thus equality (14), neglecting $o_1(\|\theta - \theta_d\|^2)$, holds true only for $(q, \theta) = (q_d, \theta_d)$.

Summarizing, locally around $(q, \theta) = (q_d, \theta_d)$ and away from kinematic singularities for a non-redundant robot, (q_d, θ_d) is a unique isolated equilibrium configuration of the closed-loop system (1), (2), (6). Indeed, local validity is an over-conservative statement and uniqueness of such equilibrium holds in the whole joint space region where q_d is the only inverse kinematics solution associated to x_d.

3.2 Proof of asymptotic stability

The stability of the proposed control law is proven by using the direct Lyapunov method and then invoking La Salle's Theorem.

Consider the auxiliary configuration-dependent function

$$\begin{aligned} P(q, \theta) &= \frac{1}{2} (q - \theta)^T K (q - \theta) + \frac{1}{2} \left(x_d - x(\tilde{\theta})\right)^T K_P \left(x_d - x(\tilde{\theta})\right) \\ &\quad + U_g(q) - \theta^T g(q_d). \end{aligned} \tag{18}$$

It is easy to see that this function, under the assumption (16), has a unique minimum in (q_d, θ_d). In fact, the necessary condition for a minimum of $P(q, \theta)$ is

$$\nabla P(q, \theta) = \begin{bmatrix} \nabla_q P \\ \nabla_\theta P \end{bmatrix} = \begin{bmatrix} K & -K \\ -K & K \end{bmatrix} \begin{bmatrix} q \\ \theta \end{bmatrix} + \begin{bmatrix} g(q) \\ -J^T(\tilde{\theta}) K_P \left(x_d - x(\tilde{\theta})\right) - g(q_d) \end{bmatrix} = 0. \tag{19}$$

Equation (19) is exactly in the form (8), (9). Using the same arguments of Section 3.1, it can be obtained that $\nabla P(q,\theta)=0$ only at (q_d,θ_d). Moreover,

$$\begin{aligned}\nabla^2 P(q_d,\theta_d) &= \left[\begin{array}{cc} K & -K \\ -K & K+J^T(\tilde{\theta})K_P J(\tilde{\theta}) \end{array}\right] + \left[\begin{array}{cc} \frac{\partial g(q)}{\partial q} & 0 \\ 0 & -\frac{\partial J^T(\tilde{\theta})}{\partial \theta}K_P\left(x_d - x(\tilde{\theta})\right) \end{array}\right]\Bigg|_{q=q_d,\theta=\theta_d} \\ &= \bar{K} + \left[\begin{array}{cc} \frac{\partial g(q)}{\partial q} & 0 \\ 0 & o_1(\|\theta-\theta_d\|^2) \end{array}\right]\Bigg|_{q=q_d,\theta=\theta_d} \end{aligned} \tag{20}$$

where the expansion (14) has been used. The sufficient condition for a minimum, i.e.

$$\nabla^2 P(q,\theta)|_{q=q_d,\theta=\theta_d} > 0. \tag{21}$$

is satisfied under the assumption (16).

The function derived from (18) as

$$V(q,\theta,\dot{q},\dot{\theta}) = \frac{1}{2}\dot{q}^T M(q)\dot{q} + \frac{1}{2}\dot{\theta}^T I\dot{\theta} + P(q,\theta) - P(q_d,\theta_d)$$

is zero at the chosen equilibrium state, $q=q_d$, $\theta=\theta_d$, $\dot{q}=\dot{\theta}=0$, and positive for any other state in an open neighborhood of this equilibrium, provided that condition (16) holds true. Hence, V is a candidate Lyapunov function.

Along the trajectories of the closed-loop system (1), (2), (6), the time derivative of V becomes

$$\begin{aligned}\dot{V} &= \dot{q}^T M(q)\ddot{q} + \frac{1}{2}\dot{q}^T\dot{M}(q)\dot{q} + \dot{\theta}^T I\ddot{\theta} + \left(\dot{q}-\dot{\theta}\right)^T K\left(q-\theta\right) - \dot{\theta}^T J^T(\tilde{\theta})K_P\left(x_d - x(\tilde{\theta})\right) \\ &\quad + \dot{q}^T\left(\frac{\partial U_g(q)}{\partial q}\right)^T - \dot{\theta}^T g(q_d) = \dot{q}^T\left(-S(q,\dot{q})\dot{q} - g(q) - K(q-\theta) + \frac{1}{2}\dot{M}(q)\dot{q} + K(q-\theta) + g(q)\right) \\ &\quad + \dot{\theta}^T\Big(u - K(\theta-q) - K(q-\theta) - J^T(\tilde{\theta})K_P\left(x_d - x(\tilde{\theta})\right) - g(q_d)\Big) \\ &= \dot{\theta}^T\Big(J^T(\tilde{\theta})K_P\Big(x_d - x(\tilde{\theta})\Big) - K_D\dot{\theta} + g(q_d) - J^T(\tilde{\theta})K_P\Big(x_d - x(\tilde{\theta})\Big) - g(q_d)\Big) \\ &= -\dot{\theta}^T K_D\dot{\theta} \le 0 \end{aligned} \tag{22}$$

where the skew-symmetry of matrix $\dot{M}-2S$ and the identity $\dot{\tilde{\theta}}=\dot{\theta}$ have been used.

Since $\dot{V}=0$ if and only if $\dot{\theta}=0$, when $\dot{\theta}\equiv 0$ the closed-loop equations give

$$M(q)\ddot{q} + S(q,\dot{q})\dot{q} + g(q) + Kq = K\theta = \text{const} \tag{23}$$

$$Kq = K\theta - J^T(\theta - K^{-1}g(q_d))K_P\left(x_d - x\left(\theta - K^{-1}g(q_d)\right)\right) - g(q_d) = \text{const}. \tag{24}$$

From (24), it follows that $\dot{q}=\ddot{q}=0$, which in turn simplifies (23) to

$$g(q) + K(q - \theta) = 0. \tag{25}$$

It has already been shown in Section 3.1 that the system (24), (25) has a unique solution, around a nonsingular (q_d, θ_d), provided that condition (16) holds true. Therefore, $q = q_d$, $\theta = \theta_d$, $\dot{q} = \dot{\theta} = 0$ is the largest invariant subset contained in the set of states such that $\dot{V} = 0$. By La Salle's Theorem, asymptotic stability of the desired set point can be concluded.

4 Compliance control with on-line gravity compensation

The control law (6) uses a *constant* gravity compensation at the desired closed-equilibrium. A better transient behavior can be expected if gravity compensation is performed at any configuration during motion. However, note that the gravity vector in (1) depends on the link variables q, which are not directly measurable. This is similar to the dependence on q of the direct and differential kinematics of the robot —see (5)— and therefore, by analogy, one can attempt using the 'gravity-biased' variable $\tilde{\theta}$, defined in (7), in place of q also for the *on-line* gravity compensation, i.e.,

$$u = J^T(\tilde{\theta}) K_P \left(x_d - x(\tilde{\theta}) \right) - K_D \dot{\theta} + g(\tilde{\theta}) \tag{26}$$

where $K_P > 0$ and $K_D > 0$ are both symmetric (and typically diagonal) matrices.

In what follows it is shown that the control law (26) provides asymptotic stability of the closed-loop equilibrium configuration (11), under the same assumption (16). The study of the closed-loop equilibria is, however, slightly different and the stability analysis requires a modified Lyapunov function candidate.

4.1 Closed-loop equilibria

The equilibrium configurations of the closed-loop system (1), (2), (26) are computed by setting $\dot{q} \equiv \dot{\theta} \equiv 0$. This yields

$$g(q) + K(q - \theta) = 0 \tag{27}$$

$$K(\theta - q) = J^T(\tilde{\theta}) K_P \left(x_d - x(\tilde{\theta}) \right) + g(\tilde{\theta}). \tag{28}$$

Following the same procedure as in Section 3.1 leads to

$$J^T(q + K^{-1}(g(q) - g(q_d))) K_P \left(x_d - x(q + K^{-1}(g(q) - g(q_d))) \right) + g(\tilde{\theta}) - g(q) = 0 \tag{29}$$

which has

$$q = q_d \quad \text{and thus} \quad \theta = q_d + K^{-1} g(q_d) := \theta_d \tag{30}$$

as a closed-loop equilibrium configuration. Moreover, in correspondence of this equilibrium, $\tilde{\theta}_d := \theta_d - K^{-1}g(q_d) = q_d$ and consequently $g(\tilde{\theta}_d) = g(q_d)$ and $x(\tilde{\theta}_d) = x_d$.

Further analysis allows showing that such equilibrium is unique. Adding to both (27) and (28) the term $K(\theta_d - q_d) - g(q_d) = 0$ and recalling expansion (14), the equilibrium equations can be rearranged as

$$\begin{bmatrix} K & -K \\ -K & K + J^T(\tilde{\theta})K_P J(\tilde{\theta}) \end{bmatrix} \begin{bmatrix} q - q_d \\ \theta - \theta_d \end{bmatrix} = \begin{bmatrix} g(q_d) - g(q) \\ g(\tilde{\theta}) - g(q_d) + o_1(\|\theta - \theta_d\|^2) \end{bmatrix}. \tag{31}$$

Assuming to be close enough to θ_d, the vanishing second-order terms can be neglected and, away from kinematic singularities, condition (16) can be assumed valid. Consequently,

$$\left\| \bar{K} \begin{bmatrix} q - q_d \\ \theta - \theta_d \end{bmatrix} \right\|^2 \geq \lambda_{\min}^2\left(\bar{K}\right) \left\| \begin{bmatrix} q - q_d \\ \theta - \theta_d \end{bmatrix} \right\|^2 = \lambda_{\min}^2\left(\bar{K}\right) \left(\|q - q_d\|^2 + \|\theta - \theta_d\|^2\right) \tag{32}$$

can be written for the left-hand side of (31), while

$$\left\| \begin{array}{c} g(q_d) - g(q) \\ g(\tilde{\theta}) - g(q_d) \end{array} \right\|^2 = \|g(q_d) - g(q)\|^2 + \|g(\tilde{\theta}) - g(q_d)\|^2 \leq \alpha^2 \left(\|q - q_d\|^2 + \|\theta - \theta_d\|^2\right) \tag{33}$$

is obtained for the right-hand side, using inequality (4) and the identity $\tilde{\theta} - q_d = \theta - \theta_d$. By comparing (32) with (33), it follows that, when $\lambda_{\min}\left(\bar{K}\right) > \alpha$, the equality in (31) is possible only for $(q, \theta) = (q_d, \theta_d)$, which is thus the unique equilibrium configuration of the closed-loop system (1), (2), (26).

4.2 Proof of asymptotic stability

Define the auxiliary configuration-dependent function

$$P(q, \theta) = \frac{1}{2}(q - \theta)^T K (q - \theta) + \frac{1}{2}\left(x_d - x(\tilde{\theta})\right)^T K_P \left(x_d - x(\tilde{\theta})\right) + U_g(q) - U_g(\tilde{\theta}). \tag{34}$$

The sole difference between Eq. (18) and (34) is in the last term $-U_g(\tilde{\theta})$ in place of $-\theta^T g(q_d)$.

As in Section 3.2, it can be demonstrated that this function has a unique minimum in (q_d, θ_d), provided that condition (16) is satisfied.

Consider the candidate Lyapunov function

$$V(q, \theta, \dot{q}, \dot{\theta}) = \frac{1}{2}\dot{q}^T M(q)\dot{q} + \frac{1}{2}\dot{\theta}^T I \dot{\theta} + P(q, \theta) - P(q_d, \theta_d) \geq 0. \tag{35}$$

Indeed, V is zero only at the desired equilibrium state $q = q_d$, $\theta = \theta_d$, $\dot{q} = \dot{\theta} = 0$.

Along the trajectories of the closed-loop system (1), (2), (26), the time derivative of V becomes

$$\begin{aligned}\dot{V} &= \dot{q}^T M(q)\ddot{q} + \frac{1}{2}\dot{q}^T\dot{M}(q)\dot{q} + \dot{\theta}^T I\ddot{\theta} + \Big(\dot{q}-\dot{\theta}\Big)^T K\,(q-\theta) - \dot{\theta}^T J^T(\tilde{\theta})K_P\Big(x_d - x(\tilde{\theta})\Big) \\ &\quad + \dot{q}^T\left(\frac{\partial U_g(q)}{\partial q}\right)^T - \dot{\theta}^T\left(\frac{\partial U_g(\tilde{\theta})}{\partial\theta}\right)^T = \dot{q}^T\left(-S(q,\dot{q})\dot{q} - g(q) - K(q-\theta) + \frac{1}{2}\dot{M}(q)\dot{q} + K(q-\theta)\right) \\ &\quad + \dot{q}^T g(q) + \dot{\theta}^T\Big(u - K(\theta-q) - K(q-\theta) - J^T(\tilde{\theta})K_P\Big(x_d - x(\tilde{\theta})\Big) - g(\tilde{\theta})\Big) \\ &= \dot{\theta}^T\Big(J^T(\tilde{\theta})K_P\Big(x_d - x(\tilde{\theta})\Big) - K_D\dot{\theta} + g(\tilde{\theta}) - g(\tilde{\theta}) - J^T(\tilde{\theta})K_P\Big(x_d - x(\tilde{\theta})\Big)\Big) = -\dot{\theta}^T K_D\dot{\theta} \le 0 \end{aligned} \tag{36}$$

where, again, the identity $\dot{\tilde{\theta}} = \dot{\theta}$ and the skew-symmetry of matrix $\dot{M} - 2S$ have been used.

The time derivative $\dot{V}$ vanishes if and only if $\dot{\theta} = 0$. Substituting $\dot{\theta}(t) \equiv 0$ into the closed-loop equations yields

$$M(q)\ddot{q} + S(q,\dot{q})\dot{q} + g(q) + Kq = K\theta = \text{const} \tag{37}$$

$$Kq = K\theta - J^T(\theta - K^{-1}g(q_d))K_P\left(x_d - x(\theta - K^{-1}g(q_d))\right) - g(\theta - K^{-1}g(q_d)) = \text{const}. \tag{38}$$

From (38), it follows that $\dot{q}(t) \equiv 0$, which in turn simplifies (37) to

$$g(q) + K(q-\theta) = 0. \tag{39}$$

As shown in Section 4.1, the system (38), (39) has a unique solution, around a nonsingular (q_d, θ_d), provided that condition $\lambda_{min}(\bar{K}) > \alpha$ holds true. By La Salle's Theorem, asymptotic stability of the desired set point can be concluded.

Notice that the sufficient condition (16) involving the gain K_P cannot be relaxed when passing from constant to on-line gravity compensation. This is because the controller employs measured quantities at the motor side, rather than the link quantities that would be needed to make independent of gravity the lower bound on K_P which is sufficient for convergence. Nevertheless, it is expected that the compliance control with on-line gravity compensation continues to work even with lower position gains. Such a feature has been verified in a number of simulations which are not reported here for brevity.

4.3 Accommodation of interaction force

In case of contact with the environment, the two control laws (6) and (26) achieve a compliant behavior during interaction. In order to gain insight into the force accommodation properties of the system, a term $J^T(q)h$ shall be added on the right-hand side of (1), where h is the vector of contact generalized forces exerted from the environment on the robot's end effector. Hence, the closed-loop system equations under control (26)

become

$$M(q)\ddot{q} + S(q,\dot{q})\dot{q} + g(q) + K(q-\theta) = J^T(q)h \tag{40}$$

$$I\ddot{\theta} + K(\theta - q) = J^T(\tilde{\theta})K_P\left(x_d - x(\tilde{\theta})\right) - K_D\dot{\theta} + g(\tilde{\theta}). \tag{41}$$

By considering a simple elastic model at the contact, i.e.,

$$h = K_e(x_e - x)$$

where $K_e \geq 0$ is the environment stiffness matrix and x_e is the undeformed rest location, at steady state ($\dot{q} \equiv 0$, $\dot{\theta} \equiv 0$) it is

$$g(q) + K(q-\theta) = J^T(q)K_e\left(x_e - x\right) \tag{42}$$

$$K(\theta - q) = J^T(\tilde{\theta})K_P\left(x_d - x(\tilde{\theta})\right) + g(\tilde{\theta}). \tag{43}$$

Assuming $g(\tilde{\theta}) \simeq g(q)$, $J(\tilde{\theta}) \simeq J(q)$ and $x(\tilde{\theta}) \simeq x(q) = x$ leads to

$$K_e\left(x_e - x\right) + K_P\left(x_d - x\right) = 0.$$

The end-effector location at the equilibrium obviously differs from x_d, while the proportional control action $K_P\left(x_d - x\right)$ balances the elastic force $K_e\left(x - x_e\right)$. Therefore, both x and h can be accommodated at steady state by means of a suitable choice of the compliance K_P^{-1}. From (42), the elastic torques due to joint deformation $K(q-\theta)$ is the combined result of the achieved contact force and of the gravity torque.

5 Experimental results

Both formulations of compliance control in the Cartesian space (i.e. with constant and on-line gravity compensation) have been tested on an 8-d.o.f. robot manipulator, named the Dexter arm [19], designed for applications of rehabilitation robotics. The robot is cable-actuated and can be regarded as a manipulator with elastic joints because of the non negligible elasticity of the cables. Experiments of regulation in the joint space with both constant and on-line gravity compensation can be found in [20].

Table 1 reports the cable stiffness coefficients for the Dexter arm. Ideally, a joint is rigid whether the elastic coefficient tends to infinity; in practice, values around 10^5 Nm/rad, as for the first two joints in Table 1, indicate a minimum level of elasticity that can be neglected, in general. In the Dexter arm, this is due to the

	Joint 1	Joint 2	Joint 3	Joint 4	Joint 5	Joint 6	Joint 7	Joint 8
Elastic coefficient	10^5	10^5	$6.34 \cdot 10^3$	$3.60 \cdot 10^3$	$2.69 \cdot 10^3$	$1.69 \cdot 10^3$	$1.23 \cdot 10^2$	$2.06 \cdot 10^2$

Table 1: *Stiffness coefficients for the joints of the Dexter arm, expressed in* Nm/rad

presence of the sole motor reduction gear box between the actuator and the link of joint 1 and joint 2. All the other joints, instead, are to be regarded as elastic, in view of the cable motor transmission.

The actuation system for cable-actuated robot manipulators consists of electrical motors which are not directly connected to the links, and a mechanical transmission system, after the gear reduction, realized by pulleys and steel cables. The consequence of cable actuation is that a mechanical coupling among the joints is present even though the number of actuators is equal to the number of d.o.f.'s, as in the Dexter arm (Fig. 2).

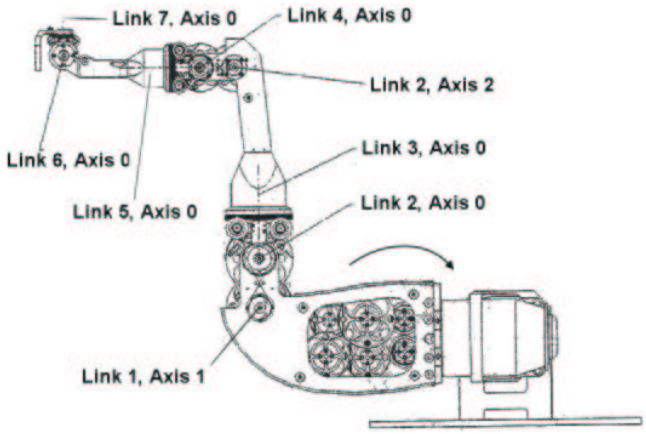

Figure 2: *The Dexter mechanical structure*

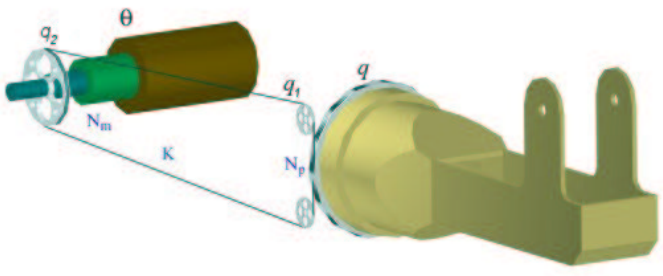

Figure 3: *A cable-actuated joint*

For the considered 8-d.o.f. robot arm, the position variables are 16, decomposed in 8 motor position values

measured by incremental encoders and 8 link position values. In Fig. 3 they are indicated respectively as θ and q, while N_m and N_P represent the matrices of gear reduction ratios and mechanical coupling, respectively.

The purpose of the experimental session is twofold. On one hand, system stability in reaching the desired position x_d is demonstrated and a comparison between control laws (6) and (26) is carried out. On the other hand, the capability of the compliance controller to modulate the level of force in the interaction is shown.

Since the robot is kinematically redundant, the effect of non-uniqueness of q_d for a given x_d on the control algorithm convergence has to be evaluated. To cope with this issue, in order to realize the task of reaching a desired position, a desired trajectory $x_d(t)$ of duration $T = 10$ s consisting of a straight-line path with a quintic polynomial time profile (with zero velocity and acceleration boundary conditions) has been planned from the robot initial Cartesian position $x_0 = [0.65\ 0\ 0.45\ 0\ 0\ 0]^T$ (m, rad) to the desired position $x_d = [0.75\ -0.06\ 0.35\ 0\ -\pi/4\ 0]^T$ (m, rad). A joint configuration trajectory $q_d(t)$ is computed off-line from $x_d(t)$ through an inverse kinematics algorithm using the pseudo-inverse of the Jacobian matrix, and initializing the scheme at the actual robot configuration at time $t = 0$. Further, the constant desired value q_d to be used in (6) or (26) and (7) is taken as $q_d = q_d(T)$.

The data reported in Figs. 4 and 5 correspond to position and orientation error in the case of constant gravity compensation and on-line gravity compensation, respectively. Both figures draw the best case from the viewpoint of accuracy, but the error of the control law (6) turns out to be larger than that of the control law (26).

The proportional matrix used for the experiments is different in the two cases. For the control with on-line gravity compensation $K_P = \text{diag}\{330, 330, 330, 12, 12, 12\}$, while for the constant gravity compensation case $K_P = \text{diag}\{120, 120, 120, 12, 12, 12\}$. For both control laws, the derivative matrix has been chosen as K_D=diag$\{10, 10, 9, 3, 2.5, 2, 0.1, 0.1\}$.

The rationale for different values of proportional gains for the position is that, if the same K_P matrix is used for the two controllers, as the motion starts, the constant gravity torque $g(q_d)$ has a higher value than that with the on-line gravity torque $g(q)$. When added to the initial error multiplied by the proportional gain K_P, this would lead to motor saturation. A reduction of K_P is thus needed for the control law (6).

Conversely, proportional gains for the orientation are unchanged because in the Dexter arm the joints responsible for the orientation have very low mass and their contribution to the gravitational torque is very

small. In spite of that, the orientation error is larger when the control law with constant gravity compensation is used, in view of the coupling with the position.

Experimental evidence shows that the closed-loop system (1), (2), (6) is stable for small displacements, whereas it can become unstable for large displacements. Moreover, accuracy for displacements along the direction of the gravity acceleration vector is higher than for displacements in the opposite direction (Figs. 4 and 6).

On the other hand, the behavior of the closed-loop system (1), (2), (26) is always stable and not influenced by the variation in magnitude or in direction of the displacement. Furthermore, the error converges asymptotically to zero and the time course of the error, in particular of the orientation error, is smoother than the case of constant gravity compensation (Figs. 4 and 5).

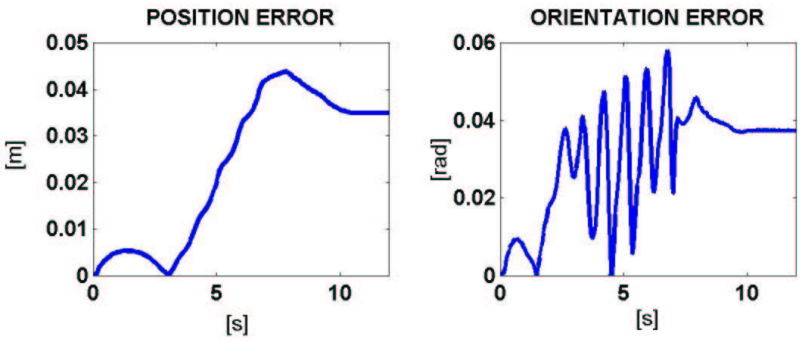

Figure 4: *Position error and orientation error in the case of compliance control in the Cartesian space with constant gravity compensation. The graph is related to a displacement in the negative vertical direction.*

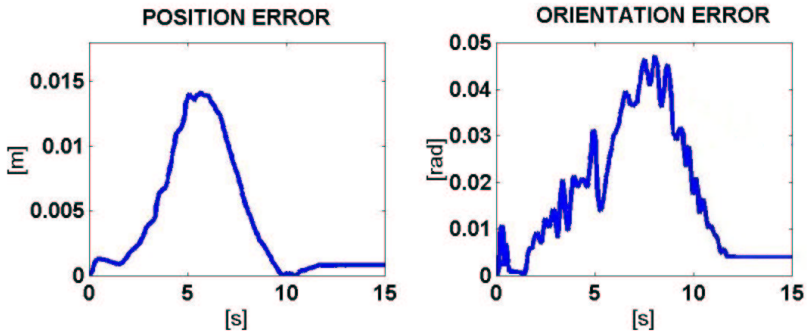

Figure 5: *Position error and orientation error in the case of compliance control in the Cartesian space with on-line gravity compensation.*

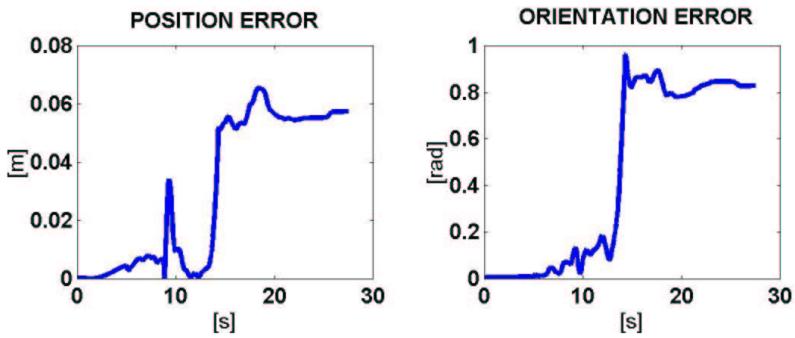

Figure 6: *Position error and orientation error in the case of compliance control in the Cartesian space with constant gravity compensation. The graph is related to a displacement in the positive vertical direction.*

In order to analyze the robot behavior in situations of interaction with the environment, the experimental setup has been equipped with an one-axis load cell, placed on an obstacle. A series of impacts have been carried out in the direction of the load cell and the contact force has been measured and monitored by means of an oscilloscope. The same procedure has been repeated for each Cartesian direction in order to evaluate the capability of the robot arm to regulate compliance in the Cartesian space.

The experiments have shown that reducing the value of K_P is a suitable means for reducing the value of the interaction force for both control laws.

Figures 5, 7 and 8 are relative to the compliance control in the Cartesian space with on-line gravity compensation and two values of K_P (i.e. K_P=diag$\{330, 330, 330, 12, 12, 12\}$ and K_P=diag$\{200, 200, 200, 6, 6, 6\}$). Figure 7 shows that decreasing K_P causes an increase of the position error, as expected. Instead, Figure 8 reports the force course during an impact in the z direction, as measured by the load cell. It is evident that a reduction of K_P corresponds to a reduction of the impact force, that is basically a regulation of robot compliance.

Further experiments, which are not reported here for brevity, have demonstrated that compliance control in the Cartesian space produces analogous results in the case of constant gravity compensation. It has been observed that the robot behavior is about the same in all the other directions of motion.

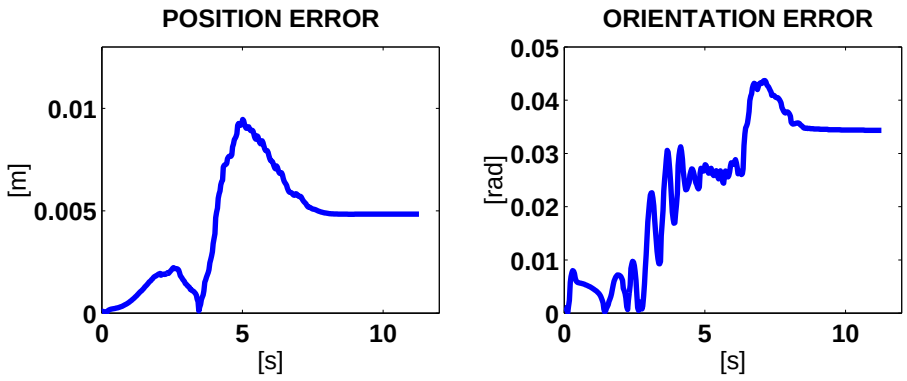

Figure 7: *Position error and orientation error in the case of compliance control in the Cartesian space with on-line gravity compensation and lower* K_P.

6 Conclusions

In designing an interaction control strategy, elasticity in the joint actuation system should not be neglected. In fact, elasticity in the joints is one of the main causes of performance degradation in tracking tasks and, whenever the robot works in contact with the environment, it is also one source of vibrational phenomena or chattering effects.

This paper has proposed a compliance control in the Cartesian space for reducing the effects of joint elasticity in the interaction. It has demonstrated that a PD action in the Cartesian space plus gravity compensation can stabilize also robots with elastic joints, by using the same sensors required for the rigid case.

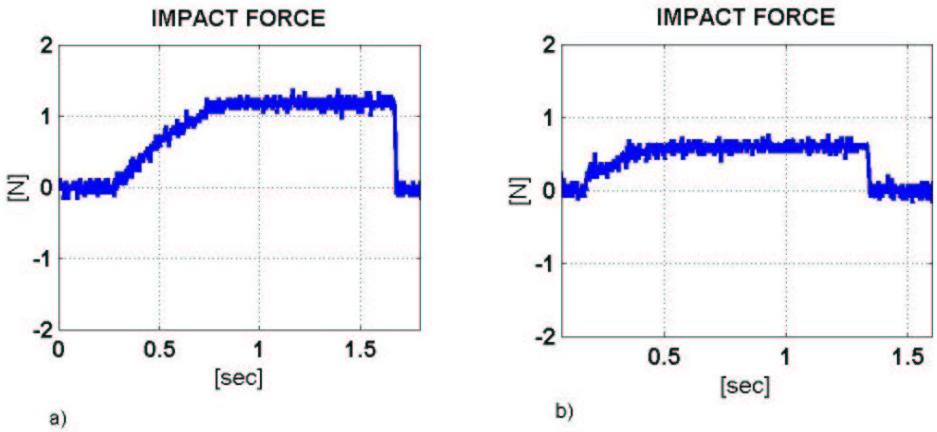

Figure 8: *Impact force in the case of compliance control in the Cartesian space with on-line gravity compensation for higher (left) and lower* K_P *values (right).*

Two formulations of the control law have been theoretically analyzed and experimentally tested. The first formulation is based on a constant gravity compensation, while the second formulation proposes an on-line

gravity compensation in order to improve robot behavior especially in the transients.

Experimental trials have been carried out on an 8-d.o.f. cable-driven robot manipulator. They have confirmed asymptotic stability of the two control laws as well as the expected improvement of transient behavior when an on-line compensation instead of a constant compensation is used for the gravity.

Further, the experimental setup has been equipped with a load cell in order to measure the exerted force in the interaction with the environment. The experimental data have revealed also the capability of compliance regulation through a suitable choice of the proportional gains.

References

[1] Zinn, M., Khatib, O., B. Roth, Salisbury, J.K., 2003, "A New Actuation Approach for Human Friendly Robot Design", in *Experimental Robotics VIII*, B. Siciliano, P. Dario (Eds.), Springer-Verlag, Heidelberg, Germany, pp. 113–122.

[2] Dario, P., Laschi, C., Guglielmelli, E., 1999, "Design and Experiments on a Personal Robotic Assistant", *Advanced Robotics*, **13**, pp. 153–169.

[3] Poulson, D., Ashby, M., Richardson, S., (Eds.), 1996, *UserFit: A Practical Handbook on User-Centred Design for Assistive Technology*, TIDE Programme, European Commission, Brussels.

[4] Dario, P., Guglielmelli, E., Allotta, B., 1994, "Robotics in Medicine", *IEEE/RSJ International Conference on Intelligent Robots and Systems*, Munich, Germany, pp. 739–752.

[5] Rivin, E.I., 1985, "Effective Rigidity of Robot Structure: Analysis and Enhancement", *American Control Conference*, Boston, MA.

[6] Sweet, L.M., Good, M.C., 1984, "Re-definition of the Robot Motion Control Problem: Effects of Plant Dynamics, Drive System Constraints, and User Requirements", *23rd IEEE Conference on Decision and Control*, Las Vegas, NV, pp. 724–731.

[7] Spong, M.W., 1989, "On the Force Control Problem for Flexible Joint Manipulators", *IEEE Transactions on Automatic Control*, **34**, pp. 107–111.

[8] Roberts, R.K., Paul, R.P., Hilberry, B.M., 1985, "The Effect of Wrist Sensor Stiffness on the Control of Robot Manipulators", *IEEE International Conference on Robotics and Automation*, St. Louis, MO, pp. 269–274.

[9] Siciliano, B., Villani, L., 1999, *Robot Force Control*, Kluwer Academic Publishers, Boston, MA.

[10] Raibert, M.H., Craig, J.J., 1981, "Hybrid Position/Force Control of Manipulators", *ASME Journal of Dynamic Systems, Measurement and Control*, **103**, pp. 126–133.

[11] Canudas de Wit, C., Siciliano, B., Bastin, G., (Eds.), 1996, *Theory of Robot Control*, Springer-Verlag, London, UK.

[12] Spong, M.W., Khorasani, K., Kokotovic, P.V., 1987, "An Integral Manifold Approach to the Feedback Control of Flexible Joint Robots", *IEEE Journal of Robotics and Automation*, **3**, pp. 291–300.

[13] Spong, M.W., 1987, "Modeling and Control of Elastic Joint Robots", *ASME Journal of Dynamic Systems, Measurement, and Control*, **109**, pp. 310–319.

[14] De Luca, A., Lucibello, P., 1998, "A General Algorithm for Dynamic Feedback Linearization of Robots with Elastic Joints", *IEEE International Conference on Robotics and Automation*, Leuven, Belgium, pp. 504–510.

[15] Tomei, P., 1991, "A Simple PD Controller for Robots with Elastic Joints", *IEEE Transactions on Automatic Control*, **36**, pp. 1208–1213.

[16] Spong, M.W., 1989, "On the Force Control Problem for Flexible Joint Manipulators", *IEEE Transactions on Automatic Control*, **34**, pp. 107–111.

[17] Mills, J.K., 1992, "Stability and Control of Elastic-Joint Robotic Manipulators during Constrained-Motion Tasks", *IEEE Transactions on Robotics and Automation*, **8**, pp. 119–126.

[18] Zollo, L., Siciliano, B., De Luca, A., Guglielmelli, E., Dario, P., 2003, "Compliance Control for a Robot with Elastic Joints", *11th International Conference on Advanced Robotics*, Coimbra, Portugal, pp. 1411–1416.

[19] Zollo, L., Siciliano, B., Laschi, C., Teti, G., Dario, P., 2003, "An Experimental Study on Compliance Control for a Redundant Personal Robot Arm", *Robotics and Autonomous Systems*, **44**, pp. 101–129.

[20] Zollo, L., De Luca, A., Siciliano, B., 2004, "Regulation with On-line Gravity Compensation for Robots with Elastic Joints", *IEEE International Conference on Robotics and Automation*, New Orleans, LA, pp. 2687–2692.

List of Figures

List of Tables